Large Synoptic Survey Telescope

www.lsst.org

Site Characterization of El Peñón: The Site of the Large Synoptic Survey Telescope

Taylor S. Chonis (U. Nebraska-Lincoln), Chuck F. Claver (NOAO), Jacques Sebag (NOAO)

El Peñón is located at the southwest end of the Cerro Pachón ridge in northern Chile. Since its selection as the LSST observatory site, detailed measurements of wind and atmospheric seeing have been conducted to help determine design and operating parameters. The wind measurements are made at 4 elevations (5, 12, 20, 30 meters) using ultrasonic 3-axis anemometers. The atmospheric seeing is monitored with a Differential Image Motion Monitor (DIMM). We have studied correlations in the wind speed and direction at the different elevations and with the atmospheric seeing. From the wind-elevation correlations, we find evidence for a surface turbulence layer up to a minimum of 12 meters above the local topography. Knowing where the boundary layer is will affect the overall height of telescope and the summit building. In examining the correlation of image quality from the DIMM with wind directions and speed, we found a surprising result: there appears to be a weak preference for better seeing when the wind is coming from the south, rather than from the northeast as expected. We also find that this correlation appears to be independent of wind speed measured to a height of 30 meters.

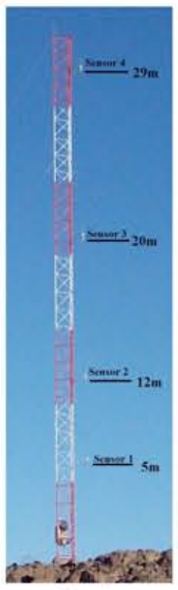

Fig. 1

I. INTRODUCTION

The Large Synoptic Survey Telescope (LSST) is an 8.4m, f/1.23 telescope equipped with a 3.2 Gpixel camera that will image a 9.62 square degree area on the sky. It is a revolutionary survey that will catalog the sky temporally *and* spatially every four days. See Ivezic et al. (2008).

For LSST to meet its goals, a high quality site is essential. Adaptive optics are not consistent over LSST's large field of view, so local site characteristics are extremely important. Cerro Pachón in Chile was chosen as LSST's site. Two years of evaluations were performed by Sebag et al. (2006). LSST's specific location on the Cerro Pachón ridge at El Peñón needs to be characterized. We wish to determine the location of the turbulent boundary layer to verify the height of the telescope (current design height is 20.5m) and to analyze wind and seeing statistics for biases that may affect the site layout.

II. EQUIPMENT & DATA

Data for this analysis is gathered from a DIMM (see Sarazin & Roddier 1990 and Tokovinin 2002) and a 30m tall wind tower, placed near each other on the summit. The DIMM is located ~5m above ground and recorded FWHM once per minute from Sept. 2007 to Mar. 2008. The wind tower is equipped with four ultrasonic 3-axis anemometers. Sensor 1, 2, 3, and 4 are located at 5m, 12m, 20m, and 29m respectively (see Fig. 1). Horizontal wind speed (*v*), vertical wind speed (*z*), azimuth wind direction (*d*), and temperature (*t*) were recorded once per second from Aug. 2007 to Apr. 2008. MATLAB is the facility for data processing and plotting.

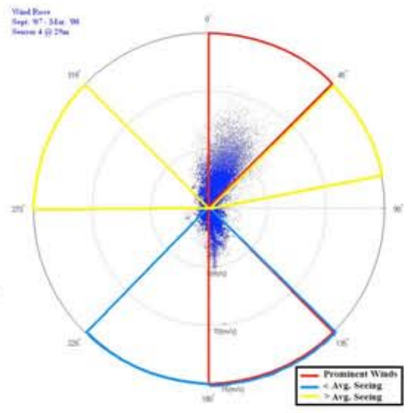

Fig. 2

III. EVIDENCE OF THE SURFACE TURBULENT BOUNDARY LAYEER

Computational fluid dynamics (CFD) models of the Cerro Pachón ridge show that the large scale topography affects a boundary layer extending up to 100m above the summit. The CFD models show the input attenuation at 30m is only 6%, meaning that at the top of the wind tower the air flow is nearly laminar. Therefore we have used Sensor 4 (at 29m) as our reference for all comparisons. We determine basic trends in wind direction and speed by plotting a standard wind rose using data from Sensor 4 for the entire data set (Fig. 2). Two dominant wind directions are present: North-North-East (62.31%) and South-South-East (20.74%). The highest wind speeds come from the North-North-East, but most wind is under 5 m/s, independent of direction.

A look at cumulative distributions of *v (Fig. 3a)*, *z (Fig. 3b)*, and *d* (Fig. 3c) shows evidence for the location of the turbulent boundary layer to be below Sensor 3. The three distributions for Sensors 3 and 4 are nearly identical while deviations Sensors 1 and 2 curves arise, indicating turbulence at those levels.

Fig. 3 Data from Sept.

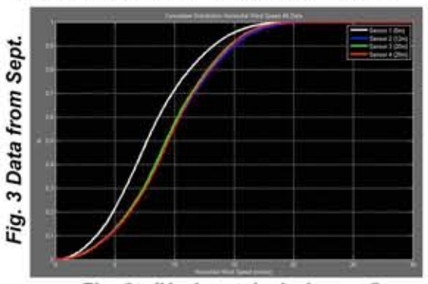

Fig. 3a (Horizontal wind speed)

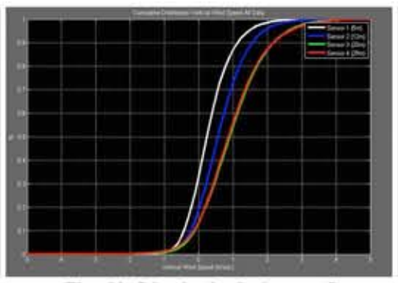

Fig. 3b (Vertical wind speed)

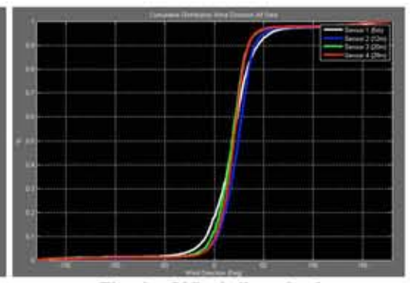

Fig. 3c (Wind direction)

Fig. 4 Data from Apr.

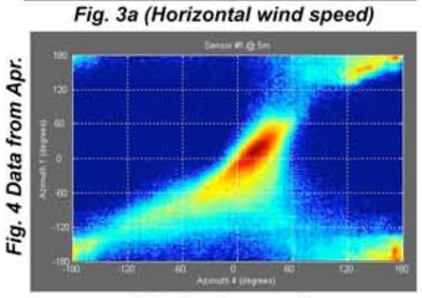

Fig. 4a (5 meters)

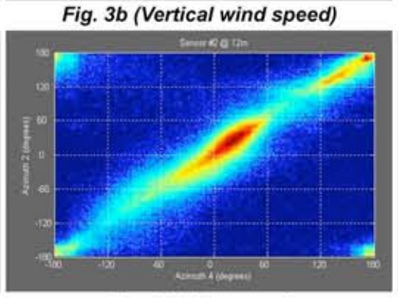

Fig. 4b (12 meters)

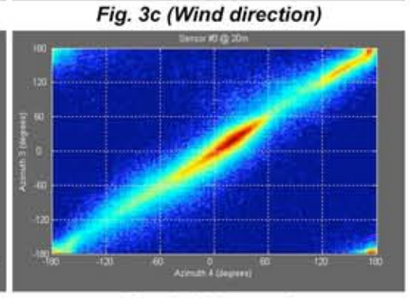

Fig. 4c (20 meters)

Stronger evidence for the surface boundary layer is found by looking at the correlations between sensor readings. Due to the large number of points, we use 2-D histograms, which are displayed as images on a log scale. Laminar flow is indicated by a strong linear correlation between sensors, weakening as laminar flow degrades. This is clearly observed in image plots (Figures 4a,b,c) for wind direction (d) for the three lower wind sensors when referenced to Sensor 4. Similarly the correlations in horizontal and vertical wind speed weaken at lower elevations as shown in Figures 5a,b,c and 6a,b,c.

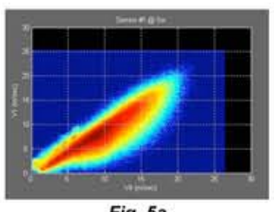

Fig. 5a (Horizontal velocity at 5m)

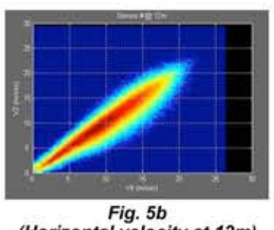

Fig. 5b (Horizontal velocity at 12m)

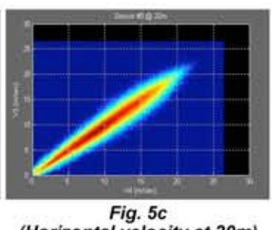

Fig. 5c (Horizontal velocity at 20m)

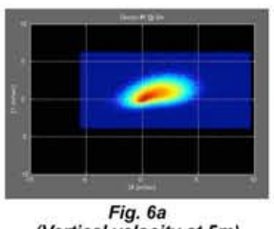

Fig. 6a (Vertical velocity at 5m)

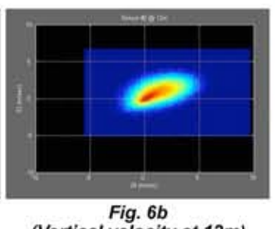

Fig. 6b (Vertical velocity at 12m)

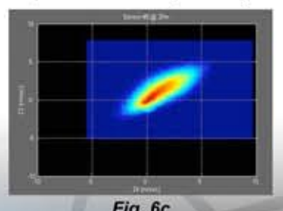

Fig. 6c (Vertical velocity at 20m)

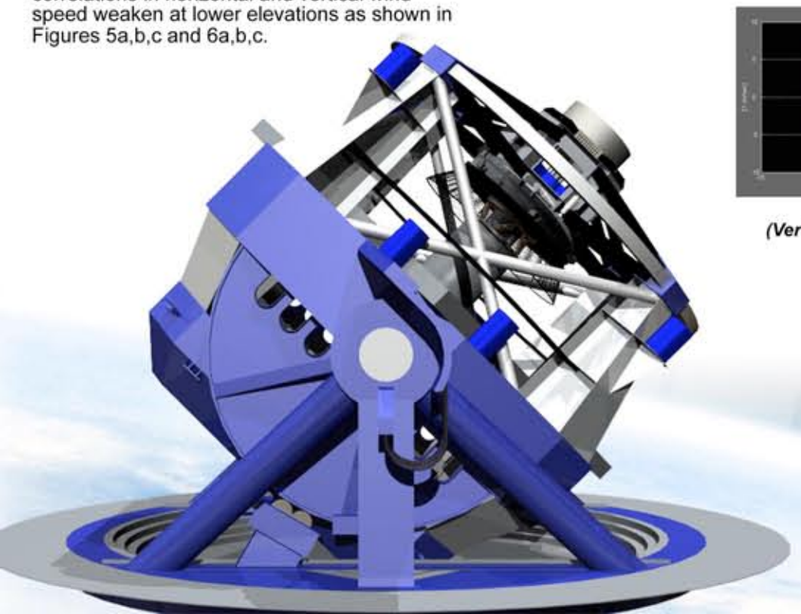

IV. CORRELATION BETWEEN SEEING & WIND PROPERTIES

The correlation between seeing and various properties of the wind are important for determining the optimal layout of the site. We plot a modified wind rose for each month; *d* is the azimuth axis, FWHM is the radial axis, and *v* is color coded (see. Fig. 7). These plots tell us several things: 1) high winds and bad seeing are correlated and appear to come out of the north; 2) highest winds occur in Sept. and Oct.; 3) High winds from dominant wind directions equalize with southern winds in Nov. to Mar. This is enforced by wind direction histograms for different months (see Fig. 8).

The plots above were preliminary and insufficient for determining biases due to over-sampling. To explore item 1 above in more detail, we proceed as follows:

- For all months, wind and seeing data are matched and compiled to one data set
- The data is divided into 25x15 degree sectors based on *d* measured by Sensor 4
- For each azimuth sector, a seeing histogram is plotted and a least squares lognormal function is fit to it; m and s are calculated (see Fig. 9)
- Once the above is done for all 24 sectors, m and s are plotted as a function of *d*

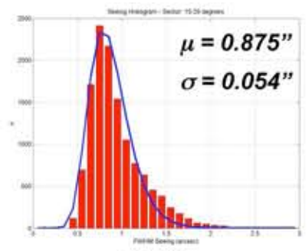

Fig. 9a

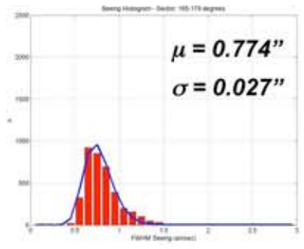

Fig. 9b

This plot for all data is shown in Fig. 10. From this, we find a surprising result: the best seeing occurs when the wind is out of the south. Over the 7 month period, 24.99% is from this direction. Areas with above average seeing happen only 6.01% of occurrences. To eliminate the possibility of this effect being due to wind shake of the DIMM, we cut the data at various wind speeds and repeat the process. No change is observed, so this effect is independent of wind speed.

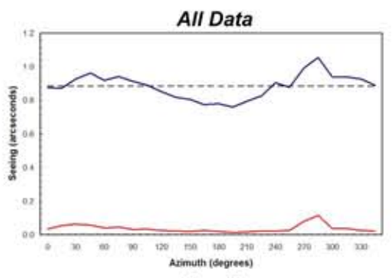

Fig. 10a

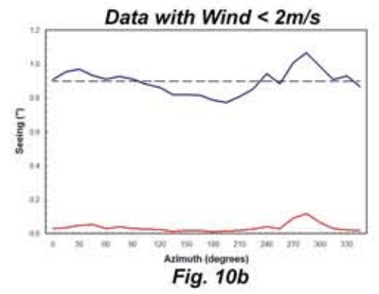

Fig. 10b

V. CONCLUSIONS

Based on the data used for this analysis, it appears that the most significant effects of the turbulent boundary layer exist below 20m, verifying the design height of the telescope. We have found seasonal trends in the wind patterns, and it seems that the best seeing occurs when the wind is from the south (see Fig. 11). This information will be used in further site layout design analysis and performance modelling of the observatory. This work is preliminary and a more complete data set must be examined before reaching conclusions about the site layout.

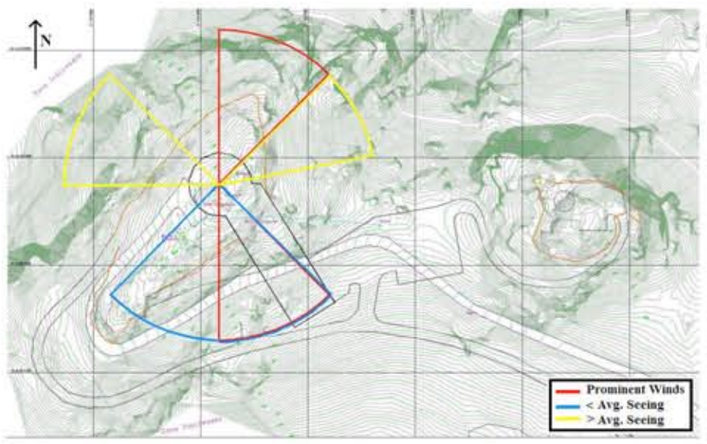

Fig. 11

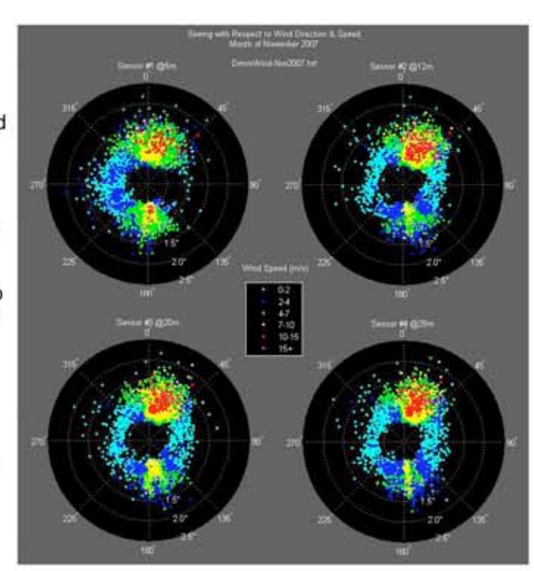

Fig. 7

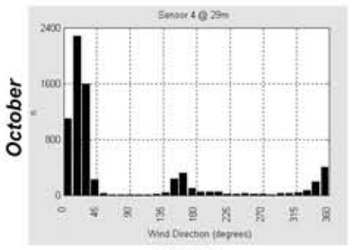

Fig. 8a

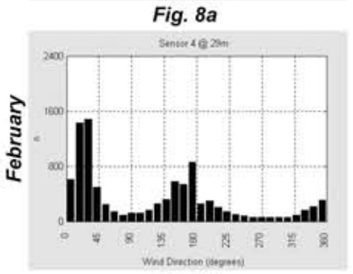

Fig. 8b

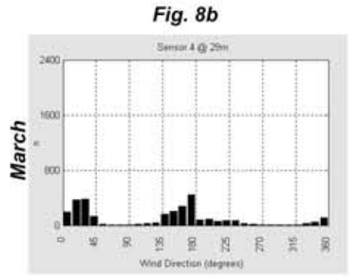

Fig. 8c

Future Work:

- Installation of micro-thermal sensors at 2m intervals to give better resolution in boundary layer height experiments.
- Extension of this data set to longer time periods is necessary for better sampling of seasonal trends.
- DIMMs and anemometers at other locations on Cerro Pachón (i.e. at Gemini South and SOAR) should be utilized to verify if the trend found in Fig. 11 is unique to El Peñón or a characteristic of the entire ridge – tells us whether this is a larger scale weather pattern.

REFERENCES

Ivezic, Z. et al. 2008, arXiv:0805.2366v1
Sarazin, M. & Roddier F. 1990, A&A, 227, 294-300
Sebag, J. et al. 2006, SPIE, 6267-57
Tokovinin, A. 2002, PASP, 114, 1156-1166

ACKNOWLEDGEMENTS

Chonis' research was supported by the NOAO/KPNO Research Experiences for Undergraduates (REU) Program which is funded by the National Science Foundation Research Experiences for Undergraduates Program and the Department of Defense ASSURE program through Scientific Program Order No. 13 (AST-0754223) and the Cooperative Agreement No. AST-0132798 between the Association of Universities for Research in Astronomy (AURA) and the NSF.